sustainability

MDPI

Article

Effect of Acetic Acid on Compressive Strength and Geometric Texture of the Surface of C20/25 Class Concrete

Joanna Witkowska-Dobrev [1], Olga Szlachetka [2,*], Marek Dohojda [1] and Krzysztof Wiśniewski [1]

[1] Institute of Civil Engineering, Warsaw University of Life Sciences—SGGW, 02-787 Warsaw, Poland; joanna_witkowska@sggw.edu.pl (J.W.-D.); marek_dohojda@sggw.edu.pl (M.D.); krzysztof_wisniewski@sggw.edu.pl (K.W.)
[2] SGGW Water Centre, Warsaw University of Life Sciences—SGGW, 02-787 Warsaw, Poland
* Correspondence: olga_szlachetka@sggw.edu.pl; Tel.: +48-22-593110

Abstract: Concrete is a highly alkaline material; therefore, the presence of organic acids (acetic, butyric, lactic) from agricultural sewage constitutes a threat to the concrete and the environment. The investigations were aimed at simulating the influence of highly concentrated organic acids on concrete elements of livestock buildings. Cubic samples 100 × 100 × 100 mm of the ordinary concrete were immersed in 10% acetic acid for 270 days. Then, the compressive strength and mass decrement of the samples were determined as well as using SEM images and a 3D-profilograph to profile the surface roughness and depth of changes evoked in the structure of the samples by penetrating acid. The results were compared with those for a control sample (not subjected to the effects of aggressive agents) as well as for samples placed in a neutral and alkaline environment. The compressive strength of the samples stored in the acidic environment was 22.23% lower than that of the control sample, whereas the compressive strength of those samples stored in an alkaline environment were 44.27% higher. Conclusions from these investigations can be of innovative importance in the preparation of environmental impact reports, which are necessary for obtaining permission for the construction and use of livestock buildings, and afterward in the reduction of the impact of these buildings on the environment and surface and underground water resources.

Keywords: livestock buildings; concrete; acidic corrosion; environmental protection; roughness analysis

check for updates

Citation: Witkowska-Dobrev, J.; Szlachetka, O.; Dohojda, M.; Wiśniewski, K. Effect of Acetic Acid on Compressive Strength and Geometric Texture of the Surface of C20/25 Class Concrete. *Sustainability* **2021**, *13*, 5136. https://doi.org/10.3390/su13095136

Academic Editors: Marzena Smol, Maria Włodarczyk-Makuła, Joanna Duda and Ludwig Hermann

Received: 12 April 2021
Accepted: 2 May 2021
Published: 4 May 2021

Publisher's Note: MDPI stays neutral with regard to jurisdictional claims in published maps and institutional affiliations.

Copyright: © 2021 by the authors. Licensee MDPI, Basel, Switzerland. This article is an open access article distributed under the terms and conditions of the Creative Commons Attribution (CC BY) license (https://creativecommons.org/licenses/by/4.0/).

1. Introduction

The deterioration of concrete elements, occurring especially in environments with reduced pH, concerns both urban and rural areas. Solutions of various acids with increased concentrations may occur mainly in industry, agriculture, or wastewater. For example, it is proved in [1] that an acid attack occurring in concrete foul sewer pipes and other sewerage components causes their significant deterioration after less than a decade in service. The concrete elements, such as dairy floors, floors and floor coverings of piggeries, the foundation of cowsheds, silage stores, and structures for collecting manure, are exposed mainly to the carboxylic acids found in agricultural effluents. Many researchers have investigated this problem, for example, [2–5]. The rate of corrosion of concrete depends on the type of acid, its concentration, pH, chemistry of the cement binder, porosity of concrete, mobility of corrosive ions, rate of flow of the corrosive medium, temperature, and pressure [6,7]. For example, mass loss and altered penetration depths are considered to be the main parameters for studying concrete degradation kinetics in a citric acid environment [8]. The corrosive action of various acids differs depending on their ability to dissociate, and the solubility of calcium salts formed after the acid reacts with the cement binder [7,9–11]. A series of papers [10,12,13] investigated the rate of corrosion of hardened cement paste with a W/C ratio equal to 0.4 in solutions of different acids—both organic, such as acetic, and formic and inorganic, such nitric, sulfuric, and hydrochloric. These

papers point out that the primary factor affecting the rate of corrosion is the solubility of the calcium salt formed after the acid reacts with the cement.

To limit the scope of this paper, the study focused on livestock buildings due to their specific environmental conditions.

In rural areas, the continuous development of animal production increases the burden on the environment [14]. This is due to, among other things, irrational management of animal faeces. The litterless system of keeping animals, widespread on industrial farms, is responsible for the formation of animal faeces in the form of liquid manure. Slurry is a source of many hazards, including excessive leakage of biogenic compounds to soils and surface and groundwater [15]. In animal and agricultural farms, decomposition of fodder or agricultural products in the presence of water leads to the formation of fodder acids (lactic, acetic, formic) with pH lower than 4.5 [2,16,17], which are the main cause of acid corrosion of concrete; because concrete is strongly alkaline, its pH is at the level of 13 [9]. The pH of silage effluent is at the level of pH = 4, while the pH of slurry and manure may vary from 6 to 8 [15]. A change in pH value entails a change in the solubility of various compounds, which may affect the stability of the concrete structure [18].

Organic acids react with hydrated and anhydrous compounds in the concrete slurry to form mainly calcium salts. Their degree of solubility determines whether these salts will precipitate or dissolve in solution. Acetic, lactic, and formic acids are examples of organic acids that are aggressive towards concrete. The main reaction between the aggressive acid medium and the concrete is the calcium hydroxide neutralization reaction, which takes place according to the general equation [11]:

$$n\mathrm{Ca(OH)_2} + 2\mathrm{H}_n\mathrm{R} \rightarrow \mathrm{Ca}_n\mathrm{R}_2 + 2n\mathrm{H_2O} \quad (1)$$

The products of this reaction are easily or poorly soluble calcium salts. The sparingly soluble salts are washed out of the cement matrix, resulting in an increase in permeability and porosity of the outer surfaces of the concrete [7,19] and a decrease in the pH of the concrete, which is related to a reduction in the amount of basic $Ca(OH)_2$ [6]. Hard-soluble salts may lack binding and strength properties, leading to a decrease in concrete strength, or they may be characterized by a larger volume than the reaction substrates, resulting in the formation of micro-cracks and, in the final stage of corrosion, destruction of the concrete [6,7,11].

Increased acid corrosion can lead to decomposition of the C-S-H phase. The first step in this process is the decalcification of the C-S-H phase, which acts as a buffer for the pore fluid. This phenomenon results in a temporary increase in the pH of the concrete, resulting in the migration of Ca^{2+} ions from the C-S-H phase into the pore fluid. The next step is the formation of an amorphous silica gel as a result of the reaction of the depleted C-S-H phase with acid according to reaction (2). The resulting amorphous gel is devoid of binding and strength properties, resulting in a reduction in the strength of the concrete [11].

$$n(x\mathrm{CaO} \cdot y\mathrm{SiO_2} \cdot z\mathrm{H_2O}) + 2x\mathrm{H}_n\mathrm{R} \rightarrow x\mathrm{Ca}_n\mathrm{R}_2 + ny\mathrm{Si(OH)_4} + n(x + z - 2y)\mathrm{H_2O} \quad (2)$$

For example, oxalic acid, which is one of the strongest carboxylic acids (pKa1 = 1.23, pKa2 = 4.19), is very little or not at all aggressive towards the concrete matrix [20]. The calcium oxalate salts formed are insoluble, which favours the protective effect of the concrete [20]. Lactic acid shows the highest aggressiveness (pKa = 3.08); this is dependent on the dissociation constant [4]. On the other hand, acids from the monocarboxylic group contained in slurry (acetic (pKa = 4.75), propionic (pKa = 4.87), butyric (pKa = 4.83)) have a similar level of aggressiveness towards concrete [4], and their effect is comparable to that of strong acids such as hydrochloric and nitric acid [17]. These monocarboxylic acids are very aggressive when coming into contact with concrete because the formed salts are highly soluble, and no protective coating, which would prevent further acid penetration into the matrix, is formed on the surface of the sample [21]. This reiterates the need for investigation of the effects of monocarboxylic acids.

This paper focuses on the effect of acetic acid. Mainly the compressive strength and the structure of the surface geometry on concrete floors in contact with 10% acetic acid are evaluated.

Tables showing typical concentrations of acetic acid occurring in real conditions can be found in [22]. In [4,18,23–25] it has been shown that acetic acid solution at pH = 4 replicates well the aggressiveness of organic acids found in animal faeces. Compared with other organic acids (butyric, lactic), acetic acid has the weakest interaction with Ca, and its salts have the highest solubility [20].

To investigate the resistance of Portland paste to acetic acid attack, samples in [21] were submerged in acetic acid solutions of 0.125 M and 0.25 M concentration for 240 days. The samples' mass and thickness changed, and pH variations of the solution were periodically monitored. The highest mass loss in the acid medium was about 2.17% in 0.125 M solution and 6.12% in 0.25 M solution. The authors rightly conclude that the evaluation of the degradation kinetics based on only mass or/and thickness change parameter is not admissible. Microstructure studies are needed to understand this phenomenon better.

The concrete samples based on CEM I 42.5N with a W/C ratio equal to 0.60 were submerged in 0.10, 0.31, and 0.52 mol/L solutions of acetic acid [17]. The 28-day compressive strength was 53 MPa, and the porosity was 12%. After 56 days of exposure to prepared solutions, the 0.7%, 2.8%, and 5% mass loss were measured, respectively. The compressive strength loss increased with the increase of acid concentration. The percentage compressive strength loss after 56 days was 13%, 18%, and 47% compared with an unexposed sample. Additionally, after 21 days, a comparison microstructure analysis of paste samples exposed to 0.52 mol/L concentration of acetic acid and just water was performed. For this analysis, the authors used a diffractometer and spectrometer. The comparison of degradation mechanisms and kinetics using EPMA, XRD, and SEM on CEM I 52.5N cement paste samples (with W/C ratio of 0.27) immersed in 0.28 mol/L concentration solutions of acetic, citric, oxalic, and tartaric acids for 360 days can be found in [26]. The main finding related to acetic acid is that this acid has an intermediate aggressiveness. This research confirmed findings from [10,12,13]: the primary parameter to consider when evaluating the aggressiveness of acids is the solubility of their salts. An acetic acid attack results in almost complete decalcification of the matrix and the dissolution of hydrated and anhydrous phases of the cement matrix. Micro-CT scanning, chemical (XRD), and mineralogical (spectrometry) analysis of the Portland cement paste exposed to acetic acid solutions of 0.1 M and 0.01 M concentration were also investigated in [27].

The results from a series of papers [25,28,29] confirm the conclusions of other researchers, but there are few studies on the effect of higher acetic acid concentration on concrete. For example, in [30], the authors evaluate the effectiveness of coating preparations used to protect ready-mix concrete with a W/C ratio equal to 0.7 against the aggressiveness of 10% acetic acid solution over a 14-day period. After 14 days of immersion in acetic solution, the compressive strength of samples with no impregnation reached 23.49 MPa. The authors do not present the change in relation to the standard compressive strength, but state that in reference to the sample protected with water glass, the value of compressive strength is lower by more than 5 MPa. Decrease of compressive strength of concrete with W/C = 0.6 made on a base of Portland cement CEM I 42.5 after storage in 10% acetic solution for 90 days at the level ca. 93% was observed in [28].

Many factors, such as the type of cement, the amount of cement, and the type of aggregate, affect the resulting properties of concrete that works in an aggressive environment [3,24]. A significant improvement in the performance of concrete in agricultural structures is achieved by improving its workability, durability, and permeability [30]. The chemical stability of the cement matrix in acidic environments can be achieved by modifying the porosity and reducing the presence of calcium hydroxide, which is most susceptible to the effects of acids [31]. Focusing on livestock buildings due to their specific environmental conditions and considering findings related to the preceding literature review, this study focused on the not-yet-well-recognized-in-literature effect of 10% acetic acid solution on

concrete floors. Mainly the compressive strength and the structure of the surface geometry were evaluated. The surface geometry evaluation included line and surface roughness measurements, which are rarely used [32,33] but seem to be a good parameter with which to evaluate the aggressiveness of acid to the concrete surface. This determination and assessment of surface roughness parameters was normalized by international ISO standards. This paper analyses which of the parameters that describe roughness sufficiently provides information about surface condition.

2. Materials and Methods

2.1. Composition of the Concrete Mixture

A concrete mix of class C20/25 and S2 consistency based on Portland cement CEM I 32.5R was designed. The proportions and amounts of components were determined based on the method of Bukowski [34]. The composition of the recipe is presented in Table 1.

Table 1. Composition of the concrete mixture.

Composite	Quantity per 1 m^3 (kg)
Cement	372.87
Water	172.09
Aggregate fraction 0–2 mm	822.79
Aggregate fraction 2–4 mm	187.00
Aggregate fraction 4–8 mm	486.20
Aggregate fraction 8–16 mm	561.00

The consistency of the concrete mixture was tested using the falling cone method, in accordance with PN-EN 12350-2 [35]. The height difference between the mould and the unformed mixture was 97 mm. After taking into account the margin of measurement error, the mix was considered to have a standard (S2) consistency. The air content, measured by the pressure method, in the concrete mixture was 1.8%, while the density of the concrete mixture was equal to 2328 kg/m^3. The W/C ratio of the designed concrete was constant and amounted to 0.5. Concretes with W/C = 0.5 are used in modern construction, e.g., in sewage treatment plant structures. The W/C value of 0.5 is important because it is the limiting level for concrete in aggressive environments. In [36] it was proved that hardened concrete paste with W/C = 0.7 exposed to an attack of acetic acid solution is expected to corrode to a depth 15% deeper than samples with W/C = 0.3 in the same period. In a nitric acid solution, the expected difference is 50%. Generally, mixtures with a W/C ratio of 0.55 and higher are treated as non-resistant to acid and chloride environments, which practically excludes them from application in the analysed conditions. The value of the W/C ratio assumed in the study under consideration is therefore adequate for checking the resistance of samples in the state of corrosive loading, and the strength values and images of microstructure should be authoritative for the assessment of the described phenomena [31].

2.2. Samples, Their Care and Seasoning

The specimens were made according to PN-EN 206+A1:2016-12 [37,38]. The samples were moulded in 100 × 100 × 100 mm moulds. After forming, the samples were stored for 24 ± 4 h in the laboratory at a temperature of 20 ± 3 °C and humidity of approximately 50%. After this time, the cubes were unmoulded and placed in a water bath for 28 days. After this period, the samples were seasoned for 270 days in a solution of 10% acetic acid (molar concentration 1.69 mol/dm^3). Additionally, two series of samples were stored in distilled water and alkaline solution (10% NaOH solution, molar concentration 5.33 mol/dm^3) for 270 days. The control sample was stored in an air-dry state in the laboratory at 20 °C and 52% humidity.

In the study, the concentration of acetic acid was higher than that which occurs naturally in livestock buildings. This allowed for a quicker assessment of the effects of

acid corrosion of concrete, the so-called accelerated method [30,39]. In order to determine the depth of acid penetration into the sample structure, various colouring pH indicators were added to the solutions [40]: methylene blue, methylene red, crystal violet, and methyl orange (Table 2, Figure 1).

Table 2. Properties of pH indicators and distilled water.

Dye	pH (–)	Conductivity (mS/dm^3)	TDS (mg/dm^3)	Temperature (°C)
Methyl blue	4.87	224	125.3	20.4
Methyl red	9.86	61.8	30.8	20.5
Crystal violet	4.51	93.8	47.4	20.5
Methyl orange	9.88	66.4	32	20.5
Distilled water	9.65	139	70.3	20.4



(**a**) (**b**) (**c**) (**d**)

Figure 1. Stained cubes [40]: (**a**) crystal violet; (**b**) methyl red; (**c**) methyl orange; (**d**) crystal blue.

The added dyes are organic compounds used as pH indicators. Blue turns green in strongly acidic solutions and blue to dark blue in slightly acidic, neutral, and basic solutions. Methyl red can change colour from dark red to pale yellow in the pH range 4.8 to 6.0. Crystal violet colours the solution violet. Methyl orange changes its colour depending on the pH of the environment it is in; in a strongly acidic environment with a pH below 3.2 it takes on a red colour, and in solutions with a pH above 4.4 it takes on a yellow colour.

The samples were placed in solution-filled containers which were tightly covered to minimise evaporation of the liquid and access of light.

2.3. Measuring pH and Salinity (TDS)

During the sample seasoning period, pH was measured weekly by potentiometry using a Hach Sension 4 m with an Ionode IJ44A gel electrode and total dissolved solids (TDS) by conductivity using a Hach Sension 156 multi-parameter meter with a 4-electrode conductivity probe with a built-in temperature sensor. Oxygen access to the test environment was only during the weekly tests. The rest of the time they were under oxygen-restricted conditions.

2.4. Compressive Strength

The compressive strength tests were performed according to the standard [37,41]. Investigations of the maximum destroying force which can be withstood by an individual sample were performed in a MATEST testing machine by loading the samples with a constant load velocity 0.6 MPa/s. The strength of an individual sample was determined according to the formula:

$$f_{c,cube(150\ mm)} = 0.95 \cdot f_{c,cube(100\ mm)} \quad (3)$$

where:

$$f_{c,cube(100mm)} = \frac{F}{Ac} \quad (4)$$

F—maximum force withstood by the sample (kN),
Ac—cross-section area of the cubic sample (mm^2).

After each trial, a destruction type (destruction cone development) was determined, aiming to confirm the test validity because any improper destruction negatively affects the correctness of the tests.

The value of the compressive strength was determined with a precision of 0.1 MPa. Assessment of the value of the compressive strength of the control sample was performed after 28 days. The compressive strength of samples seasoned in acidic, neutral, and basic solutions was measured after 270 days.

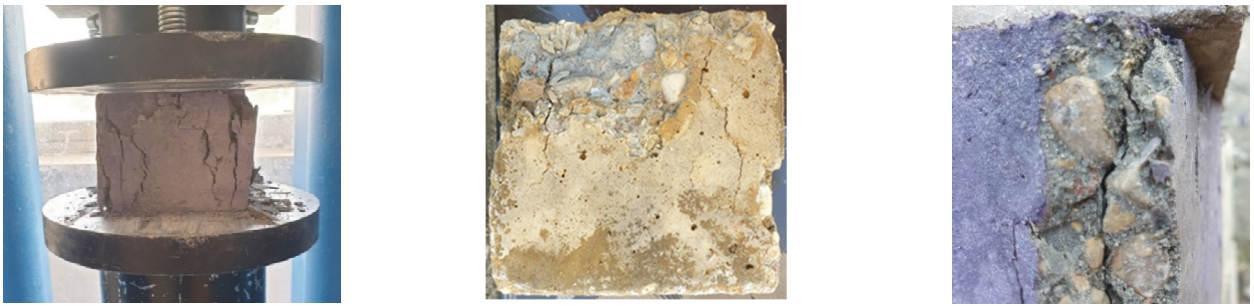
2.5. Microscopic Analysis of Sample Surfaces

Concrete samples were subjected to microscopic surface testing with the use of a Keyence digital imaging microscope of the VHX-6000 series, with a universal zoom lens VH-Z20R/Z20T and Keyence wide-area 3D measurement system VR-5000 series. The digital imaging microscope allowed the observation and assessment of the magnitude of existing micro-damage and surface topography. Images from the wide-area 3D measurement system allowed evaluation of the line and surface roughness measurement in accordance with ISO 4287 [42] and ISO 25178 [43] standards. The imaging with use of the digital microscope was supplemented with investigations using a scanning electron microscope (SEM). The SEM images were created with a scanning electron microscope FEI Quanta 200 ESEM 14-30 kV with 0.20–30 kV of accelerating voltage. The specimens for the microscope analysis measured 40 mm by 40 mm by 25 mm and were cut out from each of the samples near the edge located in direct contact with the tested environment.

3. Results and Discussion

3.1. pH, Salinity (TDS), and Compressive Strength

The samples were removed from the solutions after 270 days. They were dried and then measured, weighed, and photographed. In order to evaluate the strength parameters, the samples were destroyed in a testing machine. Figure 2 shows the samples after destruction in the testing machine.



(**a**) (**b**) (**c**)

Figure 2. View of damaged concrete samples with traces of technical dyes (**a**) with methyl red; (**b**) with methyl orange; (**c**) with crystal violet, [40].

Thanks to the use of dyes, the penetration of the solution into the sample was clearly visible. The depth of penetration of the acid into the sample could be best observed organoleptically on samples stained with methyl orange (Figure 2b). The surface of the samples was deformed in places, with clear surface defects. The greatest measured depth of acid penetration assessed on the basis of the depth of colouring was 3.8 mm.

For samples treated with a neutral pH solution with crystal violet, a strong violet colouration of only the outer surface of the cube was perceptible.

Figure 3 shows the results obtained from measuring the compressive strength of the concrete specimens in different environments, while Figure 4 compares the initial and final density of these specimens (after 270 days).

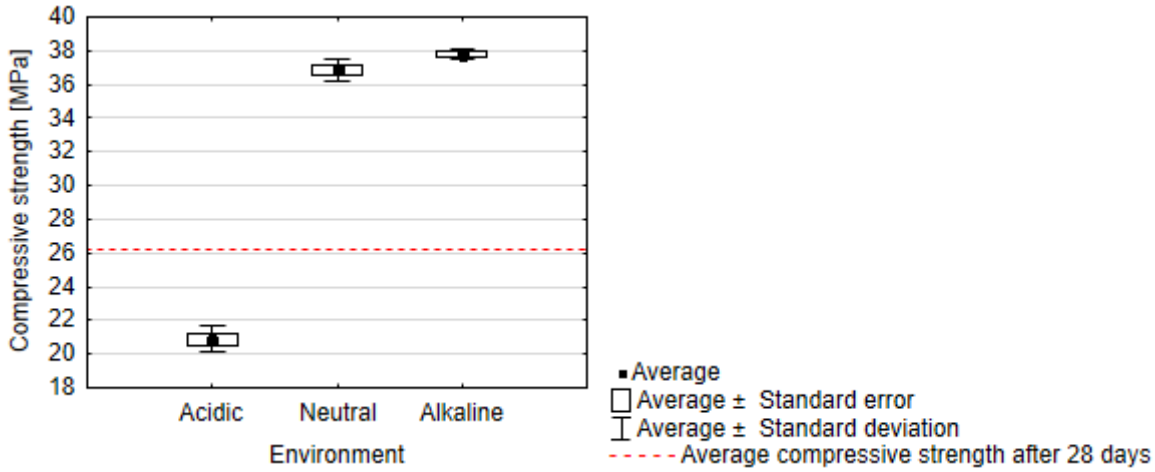


Figure 3. Boxplot of compressive strength values in different environments related to average compressive strength determined acc. [41] after 28 days.

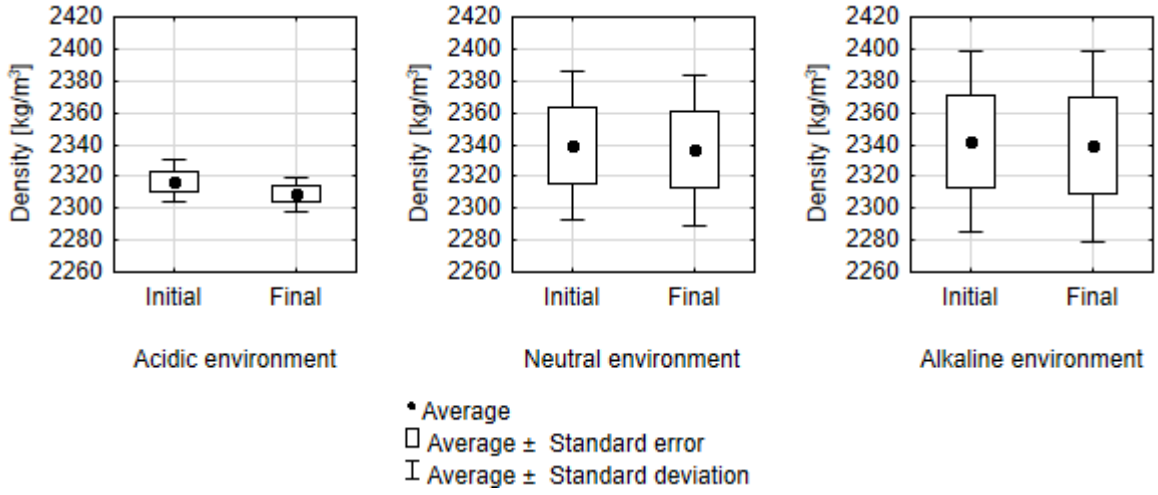


Figure 4. Comparison of boxplots of initial and final density of the concrete specimens in different environments.

The average compressive strength of the samples stored for 270 days in the acidic environment decreased in relation to the average compressive strength measured after 28 days (standard) by 22.23%, while the average compressive strength of the samples stored in the neutral and alkaline environment for 270 days increased by 40.85% and 44.27%, respectively. The reported 22% decrease in compressive strength of Portland cement-based specimens does not seem to be large at all because research results presented in [17] show that after 56 days of storage the decrease in compressive strength may be as high as 47% in relation to the standard strength in concrete specimens made from Portland cement stored in acetic acid with a concentration of 0.52 mol/L (here it was 50 MPa). The mentioned role of the W/C ratio is visible here. Concrete from [17] was characterized by a W/C equal to 0.6, which means that this concrete was more porous and thus more exposed to acid, and this caused a greater decrease of compressive strength.

The acceleration of compressive strength in a neutral and alkaline environment was expected. Due to the pH > 7, the hydration process was carried out without disturbances in the neutral environment, which favoured the development of compressive strength. The

NaOH solution provided a higher alkaline environment and higher OH- concentration in pore water, which can additionally stimulate the hydration reaction between cement components and result in the formation of hydrated products, such as CSH and CAH. It leads to a compressive strength increase. Similar conclusions related to the unconfined compressive strength of cement-solidified/stabilized soil immersed for 90 days in 1 mol/L NaOH solution can be found in [44]. The unconfined compressive strength of samples increases there by ca. 178%. Such a big improvement in unconfined compressive strength was the result of the penetrative OH- stimulating the hydration reaction between cement components and soil minerals.

The density of samples stored in an acidic environment changed the most—it decreased by 8.1 kg/m^3. Samples stored in neutral and alkaline environments lost much less mass—the difference between the initial and final densities was 3.0 and 3.1 kg/m^3, respectively. The average mass loss expressed as a percentage for samples from an acidic environment was 0.4%; for samples from a neutral environment, it was 0.1%. In the case of samples from alkaline environments, two samples lost mass on average by 0.4%, and three samples increased their mass on average by 0.1%. The recorded differences in mass of samples before and after treatment with 10% acetic acid (1.68 mol/L) are small in relation to, e.g., the study in [17], where Portland cement samples treated with 0.52 mol/L acetic acid after 56 days lost 5% of their mass, or the study in [21], where they lost 6.12%, also after 56 days in acetic acid but with concentration of 0.25 mol/L.

Figures 5–7 show the partial results of the pH and salinity (TDS) measurements of the solutions in which the samples were present. Figure 8 shows the averaged results from all 22 measurements, and Table 3 shows the coefficient of variation values for pH and salinity (TDS) values.

Table 3. Coefficient of variation (CV) pH and salinity (TDS).

Environment	CV for pH	CV for TDS
Acidic	20.59	20.62
Neutral	4.00	5.10
Alkaline	2.21	4.44

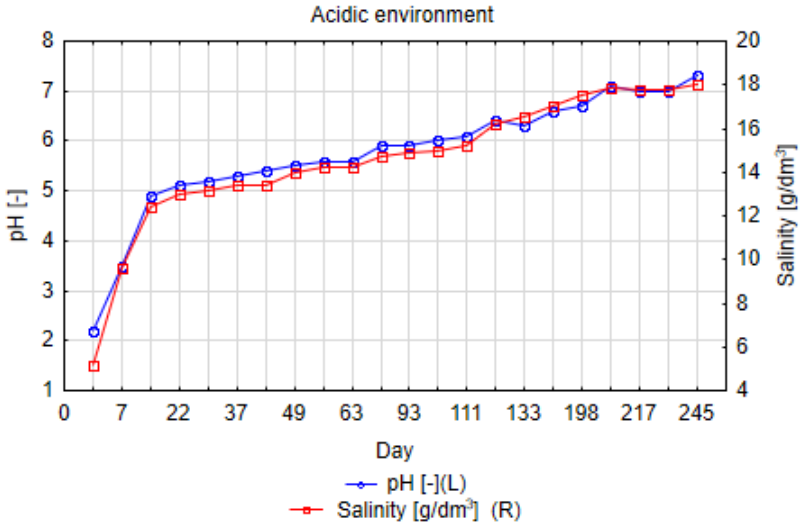


Figure 5. Decomposition of pH and salinity of acidic environments without dye.

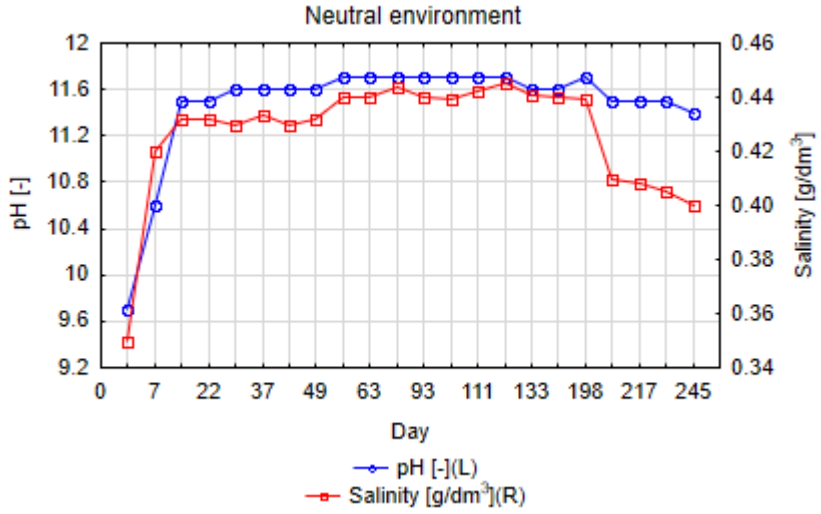


Figure 6. Decomposition of pH and salinity of an inert environment without dye.

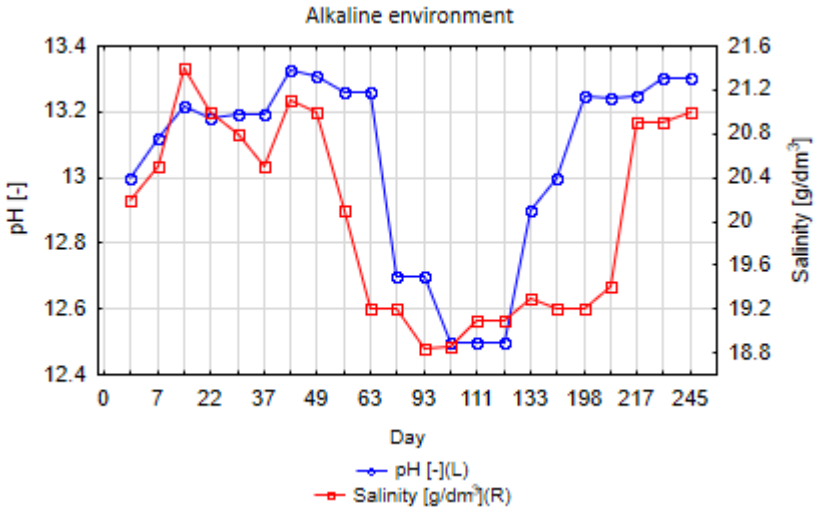
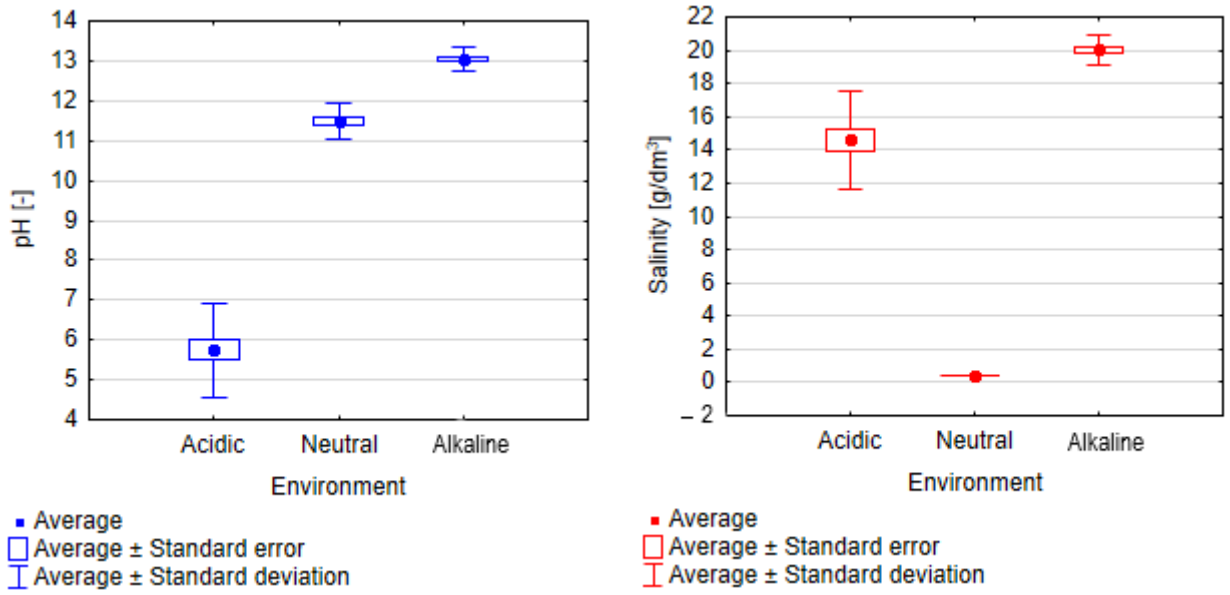


Figure 7. Decomposition of pH and salinity of alkaline environments without dye.

In the case of an acidic environment, no stabilisation of pH and salinity values was observed. The increasing trend of salinity and pH in Figure 5 indicates mineralisation of organic compounds in the acetic acid solution [45].

In the neutral environment (in distilled water), the average salinity value was 43 g/dm^3, pH was 11.47, and the coefficients of variation of these values were 4.40 and 5.10, respectively. In the alkaline environment, both pH and salinity were stable—the coefficients of variation were 2.21 and 4.44, respectively. By keeping the pH of the solution high we do not change the pH of the concrete sample. The alkaline nature of the environment further enhances quantitative alkalinisation with sodium hydroxide. The resulting poorly soluble salts did not reach a large volume and did not noticeably damage the concrete structure.

Due to the decrease in strength, the decrease in the weight of the specimens, and the presence, visible in Figure 2, of cavities and pits on the surface of the tested concrete, it can be concluded that acid corrosion took place under reduced pH conditions [3,26,27].



(**a**) (**b**)

Figure 8. Boxplots of pH and salinity measurements in different environments: (**a**) pH; (**b**) salinity (TDS).

3.2. Surface Analysis

Strength tests of concrete performed after 270 days were supplemented with an analysis of the surface of the samples using a scanning electron microscope and a 3D optical profilograph. Microscopic investigations, integrated with durability studies, enabled a diagnosis of the process of concrete surface deterioration as a result of progressive acid corrosion process [5,18,46]. Photographs taken with a 3D optical profilograph proved to be the most spectacular. The 3D profilograph presents an image with high colour contrast, which facilitates interpretation of the obtained measurement results and enables measurement of the surface roughness.

Surface roughness is characterised by fine, medium, or large texture irregularities and by surface defects spaced relatively close together or spaced in a highly random manner.

In industrial practice as well as in research, 2D (and increasingly 3D) parameters are used to quantitatively assess the condition of surfaces. Spatial parameters are more accurate than their 2D counterparts, and at the same time they are more illustrative and easier to interpret. Below we present photographs of tested samples from acetic acid solution in neutral and alkaline environments taken with a 3D microscope, along with measurements of 2D and 3D roughness parameters.

Figure 9 shows photographs of specimens seasoned in each environment, together with 3D models showing the geometric structure of the analysed surface.

Figure 10 shows the surface profiles along the selected profile lines indicated in Figure 9a–c by the blue line. The horizontal coordinate is parallel to the intersection edge of the plane tangent to the surface, and the vertical coordinate is perpendicular to this plane. Based on the determined profiles, the linear roughness parameters of the samples were determined [42] and are summarised in Table 4.

Table 4. Summary of surface geometric structure parameter values according to profile lines from Figure 10 and their comparison with the values for the air-dry sample.

Environment	Ra (μm)	Rz (μm)
Acidic	14.273	80.081
Neutral	9.143	44.831
Alkaline	4.817	23.208
Air-dry	1.927	9.288

Two basic height parameters of the surface profile were determined, i.e., the arithmetic mean of ordinates of the roughness profile (Ra) and the highest height of the roughness profile (Rz). The maximum height of the profile Rz is defined as the sum of the height of the highest elevation of the profile and the depth of the lowest depression of the profile within an elementary section. The arithmetic mean of the profile ordinates Ra is defined as the arithmetic mean of the absolute values of the ordinates within an elementary section. Both parameters have a significant influence on functional properties such as strength, tightness, and surface "wear". The Ra parameter for the samples increased by 149.97% in an alkaline environment, by 374.47% in a neutral environment, and by 640.68% in an acidic environment in relation to the value for the sample stored in the air-dry state in the laboratory at 20 °C and 52% humidity.

Comparing the measurement results obtained (see Table 4, Figures 9 and 10), the sample from the acidic environment is characterized by the highest topographic differentiation—numerous mass losses densely distributed on the sample surface are visible in the 3D image (Figure 9d–f). The sample seasoned in an alkaline medium is characterized by the lowest roughness.

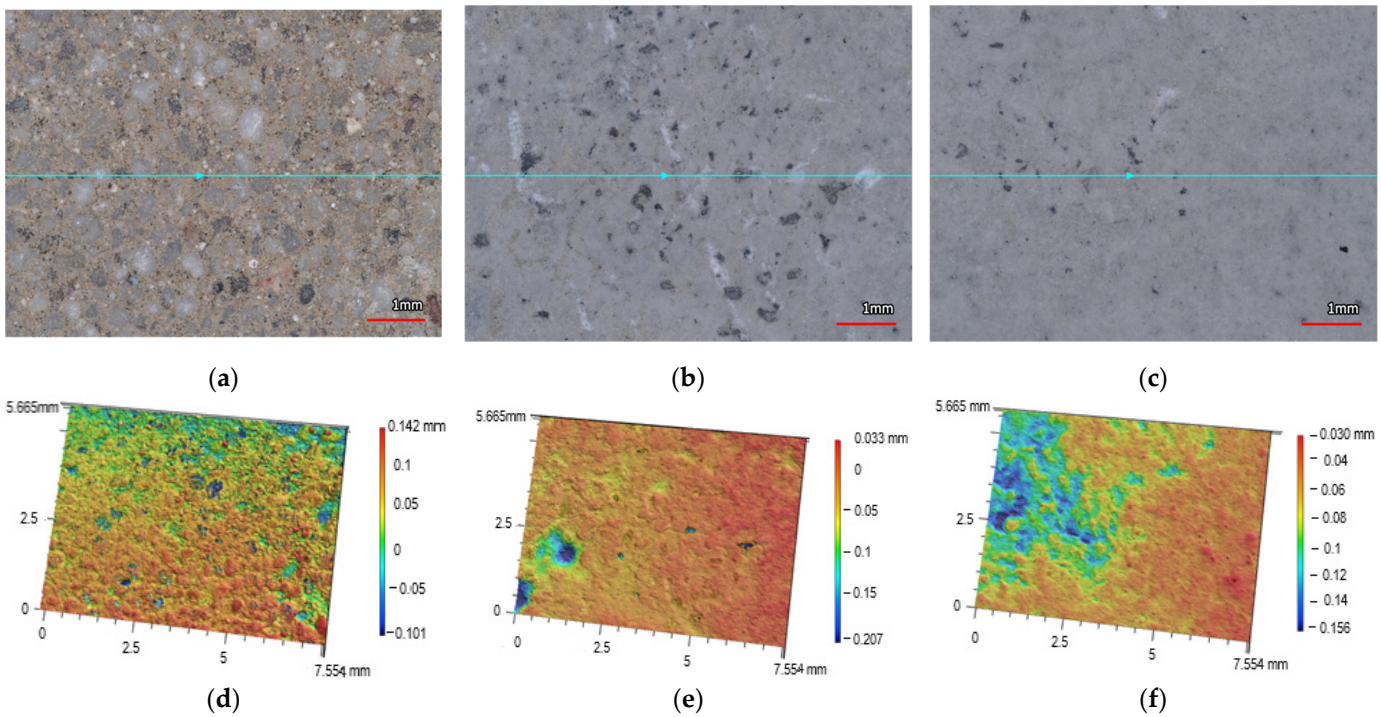


Figure 9. Photographs of samples with plotted profile lines (blue lines): (**a**) in acidic environment; (**b**) in neutral environment; (**c**) in basic environment; and geometrical structure of the analysed sample surfaces in 3D (**d**) in acidic environment; (**e**) in neutral environment; (**f**) in basic environment.

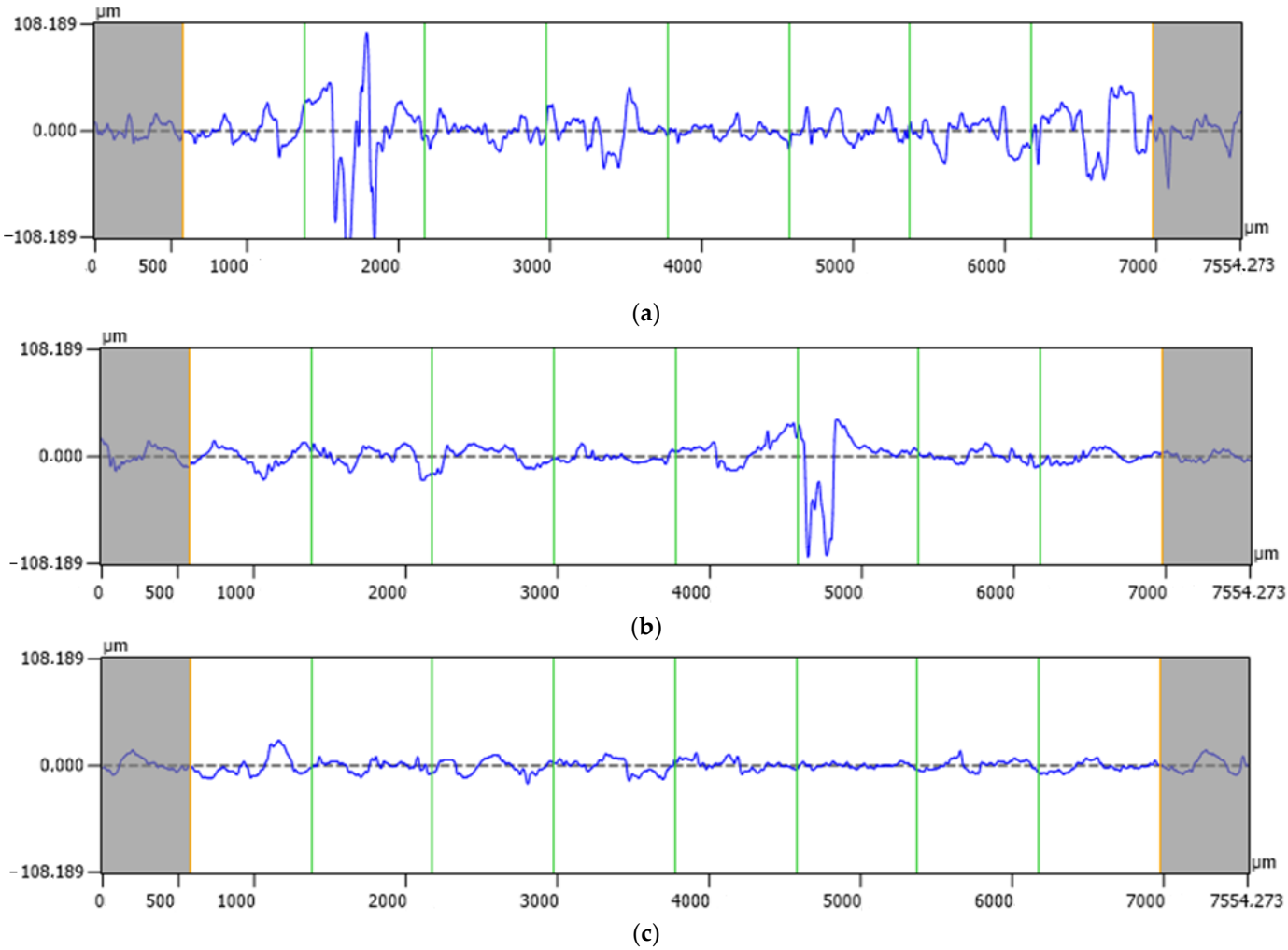


Figure 10. Roughness profiles along the profile lines (blue) from Figure 9a–c: (**a**) in acidic environment; (**b**) in neutral environment; (**c**) in basic environment.

Roughness measurements of the samples were extended by 3D parametric surface analysis according to the standard [43]. The results of this analysis are presented in Table 5.

Table 5. Summary of surface roughness parameter values.

Parameter	Acidic Environment	Neutral Environment	Alkaline Environment	Air-Dry
Arithmetical mean height of the surface Sa (µm)	23.39	11.45	5.96	2.75
Maximum height of the surface Sz (µm)	179.39	76.81	39.53	16.89
Root mean square height of the surface Sq (µm)	29.75	13.95	7.21	4.23
Skewness of height distribution Ssk (-)	−0.11	0.01	0.11	0.02
Kurtosis of height distribution Sku (-)	3.07	2.55	2.42	2.12
Maximum height of peaks Sp (µm)	82.11	39.15	23.44	10.13
Maximum height of valleys Sv (µm)	97.28	37.67	16.09	6.76

The measured areas had a surface area of about 400,000 μm^2. The analysis shows that the average values of the surface parameters change depending on the environment in which the concrete samples were seasoned. Both the height and amplitude parameters are the highest for samples cured in an acidic environment and the lowest for samples cured in a basic environment.

The Sa parameter for the samples increased by 116.73% in an alkaline environment, by 316.36% in a neutral environment, and by 750.54% in an acidic environment, compared with the value for the sample stored in the air-dry state in the laboratory at 20 °C and 52% humidity.

The structure studies were complemented by SEM images. In the images presented in Figure 11, it can be observed that in the surface layer of the fracture there are numerous cavities of various sizes, depressions and cavities confirming the destructive action of acetic acid.



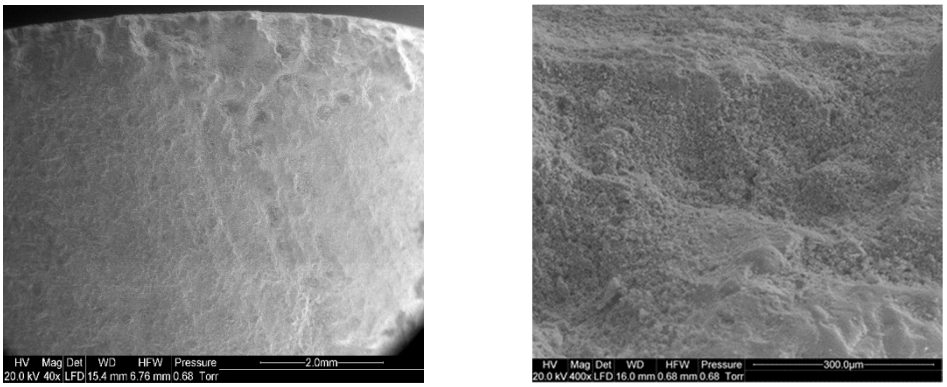
(**a**) (**b**) (**c**)

Figure 11. SEM images of a sample seasoned in an acidic environment: (**a**) edge of sample (40× magnification); (**b**) corner of sample (40× magnification); (**c**) 400× magnification.

Deformation of the surface could be observed along with localised indented traces of the acid interaction. Figure 11a,b shows areas right at the edge of the specimen with a clearly visible layer of damaged concrete structure after contact with acetic acid. A non-uniform and fragmented concrete matrix is also noticeable (Figure 11c).

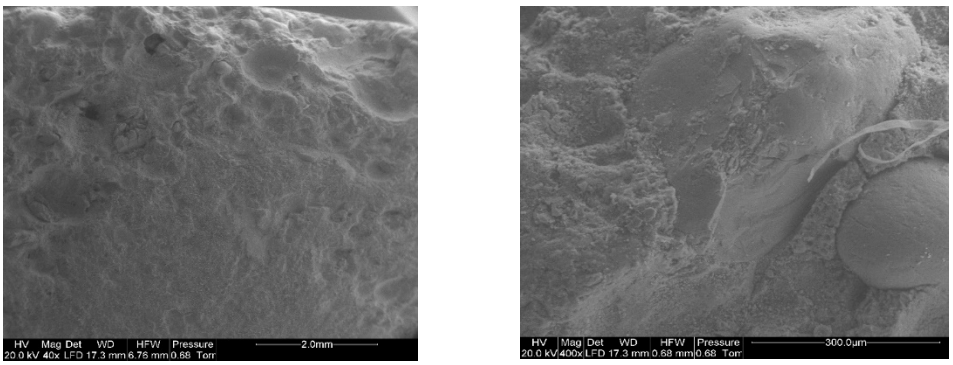
Figures 12 and 13 show images of concrete seasoned in neutral and alkaline environments, respectively. No changes or losses are visible in the images shown.

Samples seasoned in alkaline solution show the least signs of damage. Figure 13a is a photograph of the edge of the sample exposed to the alkaline solution, the area of alkali influence in the form of slight depressions, and aggregate spots can be seen here. Figure 13b shows a section of aggregate grains.



(**a**) (**b**)

Figure 12. SEM images of a sample seasoned in an inert medium: (**a**) 40× magnification; (**b**) 400× magnification.



(**a**) (**b**)

Figure 13. SEM images of the sample seasoned in alkaline medium: (**a**) 40× magnification; (**b**) 400× magnification.

4. Conclusions

In the assessment of concrete structure degradation, the dominant type of chemical corrosion occurring in livestock buildings is acid corrosion caused by organic acids. The research carried out was to check the effect of different exposure environments of concrete class C20/25 on its compressive strength, while controlling its density in the environment of chemical pigment, as an indicator of the depth of penetration of a 10% acetic acid solution.

The decrease in strength and visible defects on the surface of the samples confirm the occurrence of corrosion process. The value of the compressive strength of concrete under the influence of concentrated acetic acid decreased by 22.23% in relation to the average compressive strength measured after 28 days of the reference samples, while in alkaline and neutral environments there was a significant increase in the compressive strength value by 44.27% and 40.85%, respectively.

Samples seasoned in an acidic medium were characterised by a higher number of defects in the surface structure. The higher the surface roughness of the samples, the lower the resistance to acid action, which results from an increase in the actual contact area between the corroding areas and the aggressive medium. The 2D and 3D height parameters of surface roughness—Ra, Rz, Sa, Sq—are the most reliable in assessing the roughness intensity of corrosion damage.

The use of pH indicators staining the solutions was an attempt to determine the depth of acid penetration into the concrete sample.

The indirect aim of the surface structure study was to demonstrate the effectiveness of the Keyence laser scanner, which was used in the study to assess the morphology of concrete surfaces. The conducted roughness tests showed that the 3D profiler used in the study, with a 4K resolution, is a useful tool for assessing the morphology of concrete surfaces. It gives the possibility of obtaining the 2D and 3D roughness parameters included in ISO 4287 and ISO 25178 standards [42,43].

Microscopic tests, integrated with strength tests, made it possible to diagnose the process of concrete destruction because of the progressive process of acid corrosion. Conclusions from the conducted research may be significant in the context of future renovation of livestock facilities' buildings and in the context of the proper determination of the concrete exposure class.

Author Contributions: Conceptualization, J.W.-D. and O.S.; methodology, M.D.; literature review, J.W.-D. and K.W.; laboratory investigations O.S., J.W.-D., and M.D.; writing—original draft preparation, J.W.-D.; writing—review and editing, J.W.-D., O.S., M.D., and K.W.; visualization, O.S.; All authors have read and agreed to the published version of the manuscript.

Funding: This research received no external funding.

Institutional Review Board Statement: Not applicable.

Informed Consent Statement: Not applicable.

Data Availability Statement: Data is not publicly available, though the data may be made available on request to the corresponding author.

Acknowledgments: We would like to thank Wojciech Mika and Konrad Witek from Keyence for their help with digital imaging and roughness measurements.

Conflicts of Interest: The authors declare no conflict of interest.

References

1. O'Connell, M.; McNally, C.; Richardson, M.G. Biochemical Attack on Concrete in Wastewater Applications: A State of the Art Review. *Cem. Concr. Compos.* **2010**, *32*, 479–485. [CrossRef]
2. De Belie, N.; Verselder, H.J.; De Blaere, B.; Van Nieuwenburg, D.; Verschoore, R. Influence of the Cement Type on the Resistance of Concrete to Feed Acids. *Cem. Concr. Res.* **1996**, *26*, 1717–1725. [CrossRef]
3. Bertron, A.; Duchesne, J.; Escadeillas, G. Accelerated Tests of Hardened Cement Pastes Alteration by Organic Acids: Analysis of the PH Effect. *Cem. Concr. Res.* **2005**, *35*, 155–166. [CrossRef]
4. Bertron, A.; Duchesne, J.; Escadeillas, G. Attack of Cement Pastes Exposed to Organic Acids in Manure. *Cem. Concr. Compos.* **2005**, *27*, 898–909. [CrossRef]
5. Maraveas, C. Durability Issues and Corrosion of Structural Materials and Systems in Farm Environment. *Appl. Sci.* **2020**, *10*, 990. [CrossRef]
6. Živica, V.; Bajza, A. Acidic Attack of Cement Based Materials—A Review. Part 1. Principle of Acidic Attack. *Constr. Build. Mater.* **2001**, *15*, 331–340. [CrossRef]
7. Dąbrowska, M. *Wpływ Popiołu Lotnego Wapiennego Na Odporoność Korozyjną Kompozytów Wykonanych z Cementu Portlandzkiego Wieloskładnikowego*; Silesian University of Technology: Gliwice, Poland, 2014.
8. Nidhu, M.S.; Sniktha, V.R.; Benny, L.; Thomas, J.; Ajay, A.; Ramaswamy, K.P. Degradation Kinetics of Alkali-Activated Mortar in Aggressive Citric Acid Environment. *IOP Conf. Ser. Mater. Sci. Eng.* **2020**, *989*, 012007. [CrossRef]
9. Oueslati, O.; Duchesne, J. The Effect of SCMs and Curing Time on Resistance of Mortars Subjected to Organic Acids. *Cem. Concr. Res.* **2012**, *42*, 205–214. [CrossRef]
10. Pavlík, V. Corrosion of Hardened Cement Paste by Acetic and Nitric Acids Part I: Calculation of Corrosion Depth. *Cem. Concr. Res.* **1994**, *24*, 551–562. [CrossRef]
11. Allahverdi, A.; Škvára, F. Acidic Corrosion of Hydrated Cement Based Materials—Part 1. *Ceram. Silikáty* **2000**, *3*, 114–120.
12. Pavlík, V. Corrosion of Hardened Cement Paste by Acetic and Nitric Acids Part II: Formation and Chemical Composition of the Corrosion Products Layer. *Cem. Concr. Res.* **1994**, *24*, 1495–1508. [CrossRef]
13. Pavlík, V. Acid Attack on Hardened Cement Paste by Acids Forming Low Soluble Calcium Salts. *IOP Conf. Ser. Mater. Sci. Eng.* **2019**, *549*, 012020. [CrossRef]
14. Schipanski, M.E.; Bennett, E.M. The Influence of Agricultural Trade and Livestock Production on the Global Phosphorus Cycle. *Ecosystems* **2012**, *15*, 256–268. [CrossRef]
15. Rodrigues, J.; Alvarenga, P.; Silva, A.C.; Brito, L.; Tavares, J.; Fangueiro, D. Animal Slurry Sanitization through PH Adjustment: Process Optimization and Impact on Slurry Characteristics. *Agronomy* **2021**, *11*, 517. [CrossRef]
16. Allahverdi, A.; Škvára, F. Acidic Corrosion of Hydrated Cement Based Materials Part 2—Kinetics of the Phenomenon and Mathematical Models. *Ceram. Silikaty* **2000**, *44*, 152–160.
17. Aiken, T.A.; Kwasny, J.; Sha, W. Resistance of Fly Ash Geopolymer Binders to Organic Acids. *Mater. Struct. Constr.* **2020**, *53*, 115. [CrossRef]
18. Barbhuiya, S.; Kumala, D. Behaviour of a Sustainable Concrete in Acidic Environment. *Sustainability* **2017**, *9*, 1556. [CrossRef]
19. Mariam Ninan, C.; Ajay, A.; Ramaswamy, K.P.; Thomas, A.V.; Bertron, A. A Critical Review on the Effect of Organic Acids on Cement-Based Materials. *IOP Conf. Ser. Earth Environ. Sci.* **2020**, *491*, 012045. [CrossRef]
20. De Windt, L.; Bertron, A.; Larreur-Cayol, S.; Escadeillas, G. Interactions between Hydrated Cement Paste and Organic Acids: Thermodynamic Data and Speciation Modeling. *Cem. Concr. Res.* **2015**, *69*, 25–36. [CrossRef]
21. Ajay, A.; Ramaswamy, K.P.; Thomas, A.V. Degradation Kinetics of Alkali-Activated Pastes in Acetic Acid. *IOP Conf. Ser. Mater. Sci. Eng.* **2020**, *989*, 012010. [CrossRef]
22. Bertron, A.; Duchesne, J. Attack of Cementitious Materials by Organic Acids in Agricultural and Agrofood Effluents. *Perform. Cement Based Mater. Aggress. Aqueous Environ.* **2013**. [CrossRef]
23. Tilman, D.; Fargione, J.; Wolff, B.; D'Antonio, C.; Dobson, A.; Howarth, R.; Schindler, D.; Schlesinger, W.H.; Simberloff, D.; Swackhamer, D. Forecasting Agriculturally Driven Global Environmental Change. *Science* **2001**, *292*, 281–284. [CrossRef]
24. Voegel, C.; Bertron, A.; Erable, B. Mechanisms of Cementitious Material Deterioration in Biogas Digester. *Sci. Total Environ.* **2016**, *571*, 892–901. [CrossRef]
25. Živica, V. Acidic Attack of Cement Based Materials—A Review Part 3: Research and Test Methods. *Constr. Build. Mater.* **2004**, *18*, 683–688. [CrossRef]

26. Larreur-Cayol, S.; Bertron, A.; Escadeillas, G. Degradation of Cement-Based Materials by Various Organic Acids in Agro-Industrial Waste-Waters. *Cem. Concr. Res.* **2011**, *41*, 882–892. [CrossRef]
27. Dyer, T. Influence of Cement Type on Resistance to Attack from Two Carboxylic Acids. *Cem. Concr. Compos.* **2017**, *83*, 20–35. [CrossRef]
28. Živica, V. Deterioration of Cement-Based Materials Due to the Action of Organic Compounds. *Constr. Build. Mater.* **2006**, *20*, 634–641. [CrossRef]
29. Taku, K.J.; Amartey, D.Y.; Kassar, T. Effect of Acidic Curing Environment on the Strength and Durability of Concrete. *Civ. Environ. Res.* **2015**, *7*, 8–13.
30. Wiśniewski, K.; Dohojda, M.; Witkowska-Dobrev, J. Ochrona Betonu Zwykłego Przed Agresywnym Środowiskiem w Budownictwie Rolniczym. *ACTA Sci. Pol. Archit. Bud.* **2020**, *18*, 83–93. [CrossRef]
31. Slama, M.B.H.; Maloufi, N.; Guyon, J.; Bahi, S.; Weiss, L.; Guitton, A. In Situ Macroscopic Tensile Testing in SEM and Electron Channeling Contrast Imaging: Pencil Glide Evidenced in a Bulk β -Ti21S Polycrystal. *Materials* **2019**, *12*, 2479. [CrossRef]
32. Perez, F.; Bissonnette, B.; Courard, L. Combination of Mechanical and Optical Profilometry Techniques for Concrete Surface Roughness Characterisation. *Mag. Concr. Res.* **2009**, *61*, 389–400. [CrossRef]
33. Santos, P.M.D.; Júlio, E.N.B.S.; Silva, V.D. Correlation between Concrete-to-Concrete Bond Strength and the Roughness of the Substrate Surface. *Constr. Build. Mater.* **2007**, *21*, 1688–1695. [CrossRef]
34. Jamroży, Z. *Beton i Jego Technologie*; Wydawnictwo naukowe PWN: Warsaw, Poland, 2015.
35. PN-EN 12350-2:2019-07. *Testing Fresh Concrete. Pat 2: Slump Test*; Comite Europeen de Normalisation: Brussels, Belgium, 2019.
36. Pavlík, V. Corrosion of Hardened Cement Paste By Acetic and Nitric Acids. Part III: Influence of Water/Cement Ratio. *Cem. Concr. Res.* **1996**, *26*, 475–490. [CrossRef]
37. PN-EN 206+A1:2016-12. *Concrete—Specification, Performance, Production, and Conformity*; Polish Committee for Standardization: Warsaw, Poland, 2016.
38. PN-B-06265:2018-10. *Concrete—Specification, Performance, Production, and Conformity. National Supplement to PN-EN 206+A1:2016-12*; Polish Committee for Standardization: Warsaw, Poland, 2018.
39. Oueslati, O.; Duchesne, J. Impact of Acetic Acid Attack on the Chemical, Physical and Mineralogical Evolution of Cement Pastes. In Proceedings of the 7th International Symposium on Cement Based Materials for a Sustainable Agriculture (CIGR International Symposium), Québec City, QC, Canada, 18–21 September 2011; Godbout, S., Potvin, L., Eds.; pp. 28–37.
40. Jurak, D. *Wpływ Korozji Chemicznej Na Wytrzymałość Na Ściskanie Betonu Konstrukcyjnego C20/25*; Warsaw University of Life Sciences: Warsaw, Poland, 2020.
41. PN-EN 12390-3:2019-07. *Title. Testing Hardened Concrete—Part 3: Compressive Strength of Test Specimens*; Polish Committee for Standardization: Warsaw, Poland, 2019.
42. PN-EN ISO 4287:1999. *Geometrical Product Specifications (GPS)—Surface Texture: Profile Method—Terms, Definitions and Surface Texture Parameters*; Polish Committee for Standardization: Warsaw, Poland, 1999.
43. PN-EN ISO 25178-600:2019-05. *Geometrical Product Specifications (GPS)—Surface Texture: Areal—Part 600: Metrological Characteristics for Areal Topography Measuring Methods*; Polish Committee for Standardization: Warsaw, Poland, 2019.
44. Liu, J.; Zha, F.; Deng, Y.; Cui, K.; Zhang, X. Effect of an Alkaline Environment on the Engineering Behavior of Cement-Stabilized/Solidified Zn-Contaminated Soils. *Environ. Sci. Pollut. Res.* **2017**, *24*, 28248–28257. [CrossRef] [PubMed]
45. Živica, V.; Bajza, A. Acidic Attack of Cement-Based Materials—A Review Part 2. Factors of Rate of Acidic Attack and Protective Measures. *Constr. Build. Mater.* **2002**, *16*, 215–222. [CrossRef]
46. Xie, Y.; Lin, X.; Ji, T.; Liang, Y.; Pan, W. Comparison of Corrosion Resistance Mechanism between Ordinary Portland Concrete and Alkali-Activated Concrete Subjected to Biogenic Sulfuric Acid Attack. *Constr. Build. Mater.* **2019**, *228*, 117071. [CrossRef]